# Flightless I Regulates Hemidesmosome Formation and Integrin-Mediated Cellular Adhesion and Migration during Wound Repair

Zlatko Kopecki[1], Ruth Arkell[2], Barry C. Powell[1] and Allison J. Cowin[1,3,4]

Flightless I (Flii), a highly conserved member of the gelsolin family of actin-remodelling proteins associates with actin structures and is involved in cellular motility and adhesion. Our previous studies have shown that Flii is an important negative regulator of wound repair. Here, we show that Flii affects hemidesmosome formation and integrin-mediated keratinocyte adhesion and migration. Impaired hemidesmosome formation and sparse arrangements of keratin cytoskeleton tonofilaments and actin cytoskeleton anchoring fibrils were observed in $Flii^{Tg/+}$ and $Flii^{Tg/Tg}$ mice with their skin being significantly more fragile than $Flii^{+/-}$ and WT mice. $Flii^{+/-}$ primary keratinocytes showed increased adhesion on laminin and collagen I than WT and $Flii^{Tg/Tg}$ primary keratinocytes. Decreased expression of CD151 and laminin-binding integrins α3, β1, α6 and β4 were observed in *Flii* overexpressing wounds, which could contribute to the impaired wound re-epithelialization observed in these mice. Flii interacts with proteins directly linked to the cytoplasmic domain of integrin receptors suggesting that it may be a mechanical link between ligand-bound integrin receptors and the actin cytoskeleton driving adhesion-signaling pathways. Therefore Flii may regulate wound repair through its effect on hemidesmosome formation and integrin-mediated cellular adhesion and migration.

*Journal of Investigative Dermatology* (2009) **129,** 2031–2045; doi:10.1038/jid.2008.461; published online 12 February 2009

## INTRODUCTION

Wound healing is a complicated and highly regulated series of cellular events that result in restoration of anatomical continuity and function of the skin. Re-epithelialization is a key process involved in wound healing and is reliant on cellular ability to dissociate anchoring attachments from the basement membrane, mediated primarily by α6β4 integrin rich hemidesmosomes, and cellular ability to interact with dermal fibroblasts and the extracellular matrix proteins (El Ghalbzouri *et al.*, 2004). Cellular migration across the wound matrix and adhesion to extracellular matrix are vital events of wound repair, which involve both integrin receptors and the actin cytoskeleton.

Remodelling of the actin cytoskeleton whether for the formation of filopodia and lamellipodia or the organization of focal adhesions and stress fibers is a key process in wound healing (Defilippi *et al.*, 1999). We have previously documented that Flii, a highly conserved member of the gelsolin family of actin-remodelling proteins is an important negative regulator of wound healing (Cowin *et al.*, 2007; Kopecki and Cowin, 2008; Adams *et al.*, 2008). Our studies revealed that *Flii*-deficient mice have improved wound healing, with increased epithelial migration and enhanced wound contraction. In contrast, *Flii* overexpressing mice have impaired wound healing with larger, less contracted wounds, reduced cell proliferation, and delayed epithelial migration. Here, we investigate the differential effect of *Flii* gene expression on keratinocyte and fibroblast adhesion and migration and its relationship with integrin receptors.

Integrin transmembrane receptors are principal cell surface adhesion receptors, which mediate cell-matrix adhesion and communication promoting the attachment and migration of cells on surrounding extracellular matrix (Berrier and Yamada, 2007). Cell adhesion molecules of the integrin family consist of 18 α and 8 β subunits which form 24 αβ heterodimers, functional integrin receptors that connect the cytoskeleton to the extracellular matrix and act both as traction sites and mechanosensors altering actin cytoskeleton dynamics (Hehlgans *et al.*, 2007). Integrin cytoplasmic domains form multi-molecular complexes with proteins involved in cell signaling and with adapter proteins which connect the actin cytoskeleton, thereby controlling the tension forces necessary for cellular movement, cell–matrix interactions and tissue organization (Hynes, 2002). Integrin receptors have also been shown to greatly mediate interactions

[1]*Women's and Children's Health Research Institute, North Adelaide, South Australia, Australia;* [2]*Molecular Genetics and Evolution Group and Centre for Molecular Genetics of Development, Research School of Biological Sciences, Australian National University, Canberra, Australian Capital Territory, Australia;* [3]*Discipline of Surgery, University of Adelaide, Adelaide, South Australia, Australia and* [4]*School of Pharmacy and Medical Sciences, University of South Australia, South Australia, Australia*

*Correspondence: Allison J. Cowin, Women's & Children's Health Research Institute, 72 King William Road, North Adelaide, Australia.*
*E-mail: allison.cowin@adelaide.edu.au*

*Abbreviations: Flii, Flightless; PBS, phosphate-buffered saline*

*Received 29 July 2008; revised 11 November 2008; accepted 8 December 2008; published online 12 February 2009*

between keratinocytes and different extracellular matrix proteins, including laminin, collagen, and fibronectin (Peltonen *et al.*, 1989). Integrin binding to extracellular ligands is mediated by conformational changes induced by the interactions of the cytoplasmic domains with cytoskeletal and signaling proteins (Hehlgans *et al.*, 2007). Moreover, following the binding of the extracellular ligand, the complex multiprotein assembly of the cytoskeletal and signaling proteins is initiated, linking the integrin to the actin cytoskeleton, conveying the signal into the cell and forming the focal adhesion sites (Hehlgans *et al.*, 2007). Integrins are involved in the activation of latent TGF-β and act as potential regulators of the Smad-signaling pathways, illustrating that these receptors are more than the simple adhesion molecules and their role in cell signaling during wound healing is becoming increasingly important (Reynolds *et al.*, 2008; Wipff and Hinz, 2008).

Hemidesmosome intermediate filament structures are multi protein complexes acting as stable adhesion sites and anchoring sites for the keratin cytoskeleton, however their assembly/disassembly during wound healing is presently unclear. Integrin chains, α3, α6, β1 and β4, combine to form three functional heterodimers, α3β1, α6β1 and α6β4, which bind laminin isoforms and have been shown to be particularly important in epidermal integrity (Watt, 2002). Laminin-binding integrin receptors have also been shown to associate with the tetraspanin CD151 which promotes cellular migration by regulating integrin trafficking (Liu *et al.*, 2007), plays an important role in wound re-epithelialization (Cowin *et al.*, 2006) and is involved in hemidesmosome assembly (Litjens *et al.*, 2006). Integrin α6β4 binds directly to CD151 to form stable adhesion sites called hemidesmosomes. Studies have also shown that deletion of integrin chains α3 and β1 result in early embryonic lethality or death soon after birth (Fassler and Meyer, 1995; DiPersio *et al.*, 1997) whereas wound healing in β1 integrin conditional knockout mice is delayed due to impaired cell migration (Grose *et al.*, 2002), hence illustrating the importance of these receptors in cellular adhesion and migration during wound repair.

Wounding represents an interesting model of cell migration where cells change from a resting to a migratory phenotype, which also involves changes in integrin expression profile and requires a dramatic re-organization of the actin cytoskeleton and junctional complexes (Kirfel and Herzog, 2004; Santoro and Gaudino, 2005). Flii co-localizes with different molecules involved in regulating cytoskeleton re-organization, including Ras and Cdc42, and has both cytoskeletal and nuclear functions suggesting its involvement in numerous different pathways (Davy *et al.*, 2000; Campbell *et al.*, 2002; Lee *et al.*, 2004). It has been speculated that Flii may link signal transduction and cytoskeletal regulation (Fong and de Couet 1999). In addition, Flii is a transcriptional coactivator with the estrogen and the thyroid receptors (Lee *et al* 2004) and studies have revealed that it interferes with transcription by competing with β-catenin and FLAP1, an activator of Tcf/Lef-dependent genes (Lee and Stallcup 2006). Using $Flii^{+/-}$, wild-type, $Flii^{Tg/+}$, and $Flii^{Tg/Tg}$ mice we provide insight into the role of Flii in wound repair and show that Flii regulates hemidesmosome formation and integrin-mediated keratinocyte adhesion, spreading an outgrowth on different extracellular matrix substrates and may modulate adhesion-dependent signaling pathways contributing to improved wound repair seen in *Flii*-deficient wounds.

## RESULTS

### *Flii* overexpressing mice have more fragile skin and impaired hemidesmosome formation

The effect of *Flii* gene expression on skin architecture was initially investigated using light microscopy. Representative images are shown in Figure 1a–d. All skin sections had intact basement membranes and regular arrangement of glands and hair follicles. However, examining the distance between the basement membrane and the panniculus carnosus which includes both the papillary and sub-dermal regions showed it was clear that *Flii* overexpressing mice had significantly thinner skin than wild-type and $Flii^{+/-}$ mice (Figure 1a–d and i). In agreement with these observations, unwounded skin of $Flii^{Tg/Tg}$ mice had significantly weaker tensile strength compared to unwounded skin of $Flii^{+/-}$, wild-type and $Flii^{Tg/+}$ mice (Figure 1j). Electron transmission microscopy revealed that *Flii* overexpressing ($Flii^{Tg/+}$ and $Flii^{Tg/Tg}$) mice had significantly decreased numbers of hemidesmosomes (21.29% and 27.97% decrease, respectively compared to wild-type, Figure 1g,h and k). In contrast, $Flii^{+/-}$ mice had increased numbers of hemidesmosomes (40.39% increase, Figure 1e and k). Although there was no significant difference in hemidesmosome structure between $Flii^{+/-}$ and wild-type mice (Figure 2), *Flii* overexpression resulted in significantly reduced number of hemidesmosomes with sub-basal dense plates (Figure 2a–h and m), and significantly shorter hemidesmosome adhesion sites (Figure 2g–h and n).

Examination of desmosomes in between basal keratinocytes in the epidermis and arrangements of collagen fibers in the dermis showed no apparent differences between all four groups (data not shown). However, although $Flii^{+/-}$ and wild-type mice showed a number of intracellular networks of dense cytokeratin tonofilaments in the epidermis and anchoring fibrils in the dermis, Flii overexpressing mice had sparse tonofilaments and a decreased network of anchoring fibrils (Figure 2i–l). Electron microscopy revealed intact basal lamina separating the epidermis from the dermal connective tissue in all groups (data not shown).

### Keratinocyte and fibroblast adhesion and spreading is regulated by Flii

Impaired hemidesmosome structure observed in response to different levels of *Flii* expression suggested that Flii might affect cellular adhesion and spreading. Keratinocytes and fibroblasts derived from $Flii^{+/-}$, wildtype and $Flii^{Tg/Tg}$ skin were seeded on three extracellular matrix substrates, laminin, collagen I and fibronectin, and the effect on adhesion was determined (Figure 3a and b). Dose-dependent effects of *Flii* were observed on all three substrates investigated. $Flii^{+/-}$ keratinocytes showed significantly increased adhesion on both laminin and collagen I compared with wild-type cells

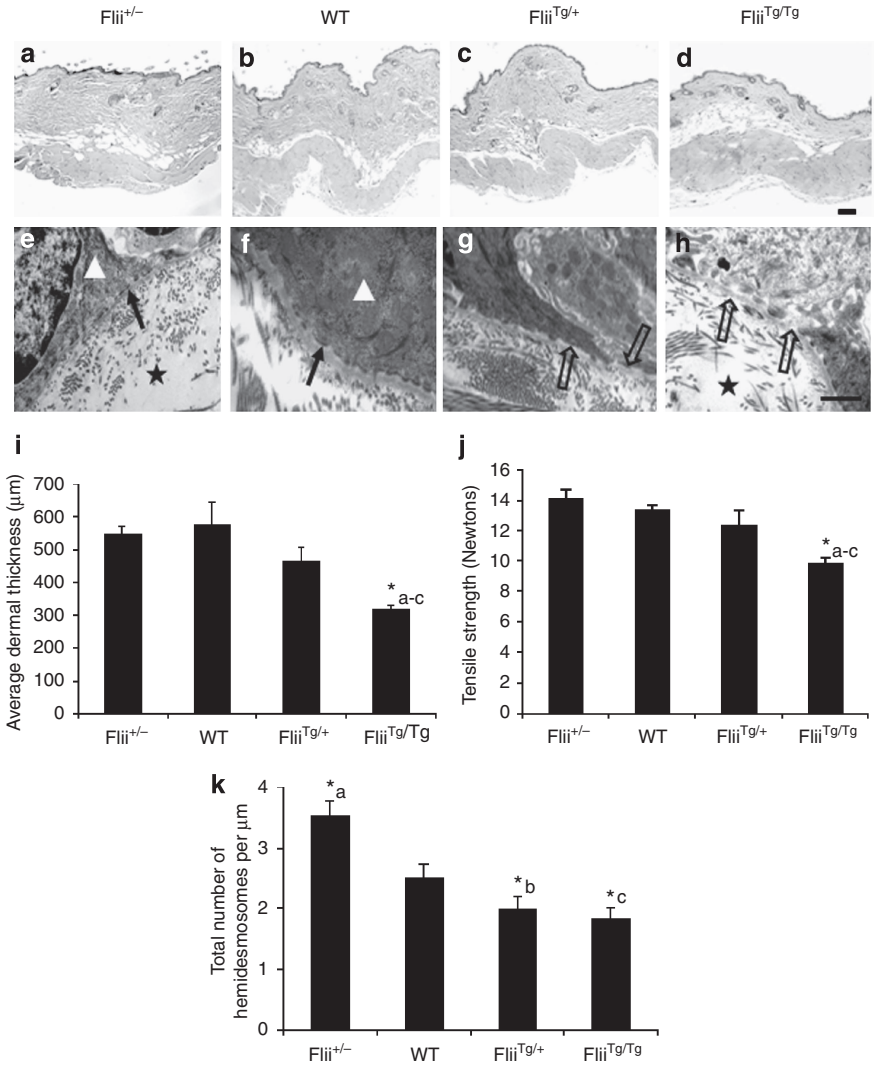


**Figure 1.** ***Flii* overexpressing mice have thinner skin and reduced hemidesmosome formation.** (**a–d**) Representative images of haematoxylin and eosin stained mice skin in $Flii^{+/-}$, WT, $Flii^{Tg/+}$, and $Flii^{Tg/Tg}$ illustrating significantly decreased dermal thickness in $Flii^{Tg/Tg}$ unwounded skin compared to other mice groups. Scale bar in D refers to A–D and = 500 μm. $n = 9$ $^*P < 0.05$. (**e–h**) Electron transmission microscopy reveals that skin from $Flii^{+/-}$ mice has significantly higher numbers of hemidesmosomes at the dermal–epidermal junction compared to WT, $Flii^{Tg/+}$, and $Flii^{Tg/Tg}$ mice. Hemidesmosomes = solid black arrow. Region without hemidesmosomes = clear arrow. Extracellular matrix = star. Basal keratinocyte = triangle. Magnification × 7900, scale bar in H refers to E–H and = 2 μm. (**i**) Graph showing effect of *Flii* gene expression on dermal skin thickness. (**j**) Tensiometer analysis of $Flii^{+/-}$, WT, $Flii^{Tg/+}$, and $Flii^{Tg/Tg}$ mice skin. $Flii^{Tg/Tg}$ mice skin had significantly weaker tensile strength compared to $Flii^{+/-}$, WT, and $Flii^{Tg/+}$ counterparts, (*a-c) respectively ($n = 12$). (**k**) Graph showing number of hemidesmosomes in unwounded skin with different levels of *Flii* gene expression. $Flii^{+/-}$ (*a) have significantly higher number of hemidesmosomes whereas both $Flii^{Tg/+}$ (*b) and $Flii^{Tg/Tg}$ (*c) have significantly decreased number of hemidesmosomes compared to *WT* counterparts ($n = 2$). All figures represent means and standard error of means $^*P < 0.05$. The color reproduction of this figure is available on the html full text version of the article.

whereas both $Flii^{+/-}$ and wild-type keratinocytes had significantly increased adhesion compared to $Flii^{Tg/Tg}$ keratinocytes on all three substrates (Figure 3a). A similar pattern of cellular adhesion was observed with primary fibroblasts where $Flii^{Tg/Tg}$ fibroblasts had significantly impaired adhesion (Figure 3b). We further examined cellular spreading on different extracellular matrix substrates by staining keratinocytes (Figure 4a–l) and fibroblasts (Figure 4m–x) with fluorescein isothiocyanate-phalloidin and examined the filamentous actin cytoskeleton organization. Defined actin rings and developed filamentous actin network were observed in $Flii^{+/-}$ and wild-type keratinocytes and fibroblasts, whereas $Flii^{Tg/Tg}$ keratinocytes and fibroblasts displayed an impaired spreading phenotype with round cell morphology and less filopodia-like processes (Figure 4a–x).

**Keratinocyte migration and cellular outgrowth are regulated by Flii**

The impact of Flii expression on keratinocyte migration (Figure 5) and cellular outgrowth on different extracellular matrix substrates was determined (Figure 6). Confluent monolayers of $Flii^{+/-}$, wildtype and $Flii^{Tg/Tg}$ keratinocyte grown on glass coverslips were scratch wounded and residual wound area examined over 48 hours. $Flii^{+/-}$ keratinocytes had a significantly improved migration and smaller wound area

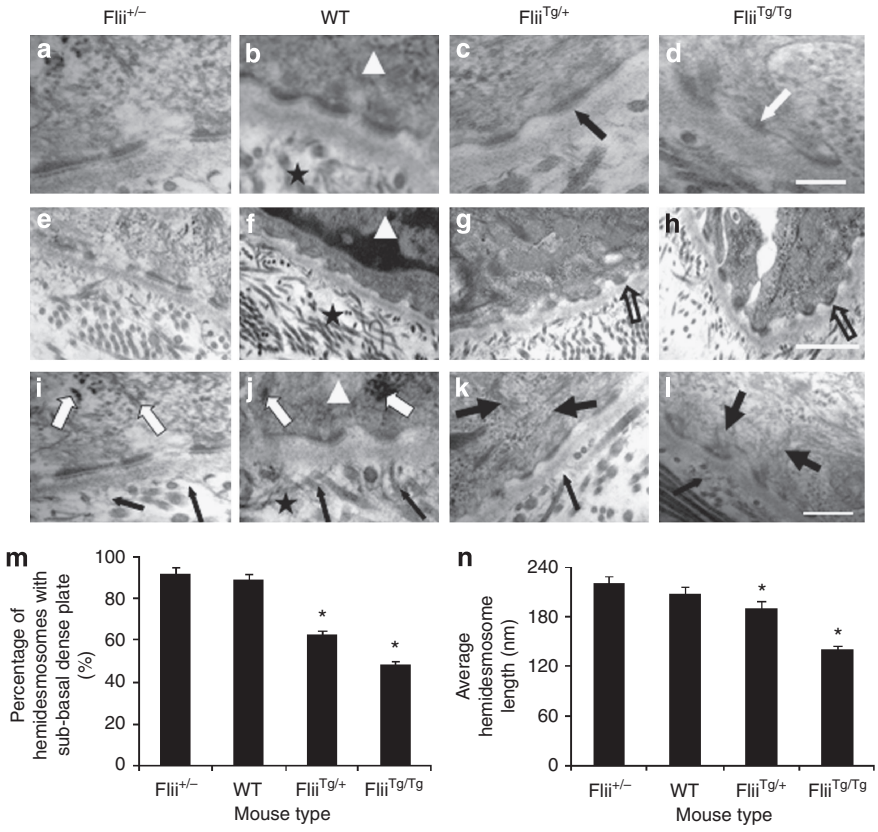


**Figure 2. *Flii* overexpressing mice have impaired hemidesmosome structure.** (**a–d**) *Flii*$^{Tg/+}$ and *Flii*$^{Tg/Tg}$ show reduced inner plaque (white arrow) and significantly decreased number of hemidesmosomes with sub-basal dense plate (black arrow). Magnification × 64,000, scale bar = 200 nm. (**e–h**) *Flii*$^{Tg/+}$ and *Flii*$^{Tg/Tg}$ mice have shorter hemidesmosomes adhesion sites (clear arrow). Magnification × 25,000, scale bar = 500 nm. (**i–l**) *Flii*$^{+/-}$ and WT mice show intracellular networks of dense tonofibrils (white arrow) and anchoring fibrils (thin black arrow) whereas *Flii*$^{Tg/+}$ and *Flii*$^{Tg/Tg}$ mice have diffuse tonofilaments (thick black arrow) and decreased network of anchoring fibrils (thin black arrow). Black star = extracellular matrix. White triangle = basal keratinocyte. Magnification × 64,000, scale bar = 200 nm. (**m**) Graphical analysis of percentage of hemidesmosomes with sub-basal dense plate. Both *Flii*$^{Tg/+}$ and *Flii*$^{Tg/Tg}$ mice have significantly reduced number of hemidesmosomes with sub-basal plate when compared to *WT* and *Flii*$^{+/-}$ mice respectively (*$P<0.05$). (**n**) Graphical analysis of hemidesmosome length. *Flii*$^{Tg/+}$ mice have significantly shorter hemidesmosome length compared to *Flii*$^{+/-}$ mice (*$P<0.05$) whereas *Flii*$^{Tg/Tg}$ mice have significantly shorter hemidesmosome length compared to *Flii*$^{+/-}$, *WT*, and *Flii*$^{Tg/+}$ mice. Figure represents means and standard error of means. One hundred and fifty hemidesmosomes measured per group, *$P<0.05$.

compared to both wild-type and *Flii*$^{Tg/Tg}$ keratinocytes (Figure 5a–d). Punch biopsy skin explants from *Flii*$^{+/-}$, wild-type, *Flii*$^{Tg/+}$, and *Flii*$^{Tg/Tg}$ mice were further used *in vitro* to determine the effect of Flii gene expression on cell migration on laminin, collagen I, and fibronectin. Results were similar on all extracellular matrix substrates investigated and representative images of cellular outgrowth from skin explants on collagen I at day 6 post culture are shown in Figure 6a. An extensive halo of cells was apparent around the explants of *Flii*$^{+/-}$ and wild-type skin after 2 days culture whereas *Flii*$^{Tg/+}$ and *Flii*$^{Tg/Tg}$ explants showed a reduced rate patchy cellular outgrowth. Although initially a mixed population of skin cells, fibroblasts rapidly became the most predominant cell type growing out of all the explants. A dose-dependent effect of *Flii* gene expression on cellular outgrowth on laminin (Figure 6b), collagen I (Figure 6c), and fibronectin (Figure 6d) was observed with *Flii*$^{+/-}$ cells migrating faster than wild type, which in turn were faster than *Flii*$^{Tg/+}$, with *Flii*$^{Tg/Tg}$ cells being the least able to migrate from the explant.

### CD151 expression is increased in *Flii*-deficient mice during wound repair

Tetraspanin CD151 is a key component of hemidesmosomes and plays an important role during wound re-epithelialization by selectively interacting with different laminin-binding integrin receptors. CD151 expression in the epidermis increased in response to wounding, peaking at day 3 and decreasing by day 7 post-wounding in wild-type and *Flii* overexpressing wounds (Figure 7a and c). In contrast, *Flii*$^{+/-}$ wounds showed significantly elevated CD151 expression at day 3 and maintained this elevated expression through to day 7 post-wounding, before returning to basal levels by day 14 post-wounding (Figure 7a–c). CD151 cellular staining within newly formed granulation tissue in the wound matrix showed no significant differences between different groups (data not shown). CD151 protein levels, as measured by western blotting, were also significantly elevated in *Flii*$^{+/-}$ wounds at both day 3 and 7 post-wounding (Figure 7b).

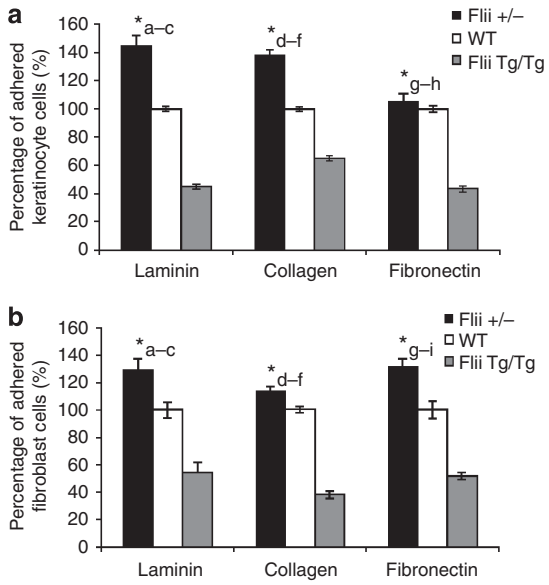


**Figure 3. Flii regulates keratinocyte and fibroblast cell adhesion.** (**a**) Graph showing keratinocyte adhesion on laminin, collagen I and fibronectin. $Flii^{Tg/+}$ keratinocytes have significantly impaired adhesion on all three substrates (*a–h), respectively. (**b**) Graphical analysis of fibroblast cell adhesion on different substrates. $Flii^{+/-}$ fibroblasts have significantly improved adhesion compared to wild-type and $Flii^{TgTg}$ counterparts on all substrates (*a–i), respectively. Figures represent a mean and standard error of means, $n=6$ $^*P<0.05$.

### Manipulation of *Flii* gene expression alters the expression of laminin and its binding integrin subunits

Laminin is a major component of the basement membrane and its processing is required for stable hemidesmosome formation and control of cellular behavior by interaction with integrin receptors in a bidirectional signaling between the extracellular matrix and the cell interior (Dogic *et al.*, 1998; Hintermann and Quaranta, 2004). Laminin protein levels, as measured by western blotting, were significantly elevated in $Flii^{+/-}$ wounds at both day 3 and 7 post-wounding (Figure 8a). The expression of laminin-binding integrin receptors are key determinants of rapid wound re-epithelialization. To explore the potential of Flii in mediating cellular adhesion and migration during wound repair, immunohistochemical analysis of laminin integrins α3, β1, α6, and β4 subunits was undertaken on $Flii^{+/-}$, wild-type, and $Flii^{Tg/+}$ wounds. Representative images of integrin α3, β1, α6, and β4 staining pattern at day 3 post-wounding are shown in Figure 8b. Integrin α3 in unwounded skin was significantly higher in $Flii^{+/-}$compared with wildtype, which in turn was higher than $Flii^{Tg/+}$. Expression was localized within both basal and suprabasal keratinocytes and wounding caused similar decreases in α3 expression in all three groups returning to baseline conditions by day 14 (Figure 9a).

The cytoplasmic domain of integrin β1 directly connects to the actin cytoskeleton and its degree of stabilization must be tightly regulated to provide optimal traction forces required for cellular migration and spreading. Integrin β1 is expressed on basal keratinocytes and its expression in response to wounding was increased in suprabasal keratinocytes along the newly forming epidermis at the wound margin returning to basal levels by day 14 post-wounding (Figure 8b and c). A dose-dependent effect of *Flii* gene expression on integrin β1 expression was observed with $Flii^{+/-}$ having a significantly elevated expression in contrast to wild-type and $Flii^{Tg/+}$, which were significantly decreased (Figure 8b and c). Similar expression was seen in fibroblasts in the wound matrix with integrin β1 expression remaining elevated until day 7 post-wounding and decreased by day 14 post-wounding (data not shown). Western blotting, confirmed this dose-dependent effect of *Flii* gene expression on β1 levels in response to wounding (Figure 8d).

Integrin α6 plays an important role in both cellular migration and adhesion during wound repair where it couples to integrin β1 and β4, during formation of a functional laminin receptor and stable hemidesmosome adhesion sites respectively (Watt, 2002). Immunostaining of $Flii^{+/-}$, wild-type, and $Flii^{Tg/+}$ mice wounds using an integrin α6-specific antibody revealed increased expression in response to wounding in all groups, with similar expression patterns in both the epidermis (Figure 8b) and wound matrix (data not shown). Integrin α6 was predominantly expressed on basal keratinocytes attached to basement membrane and on fibroblasts of newly formed granulation wound tissue (Figure 8b). No significant difference in integrin α6 expression was observed between wild-type and $Flii^{Tg/+}$ wounds at day 3 post-wounding; however, wild-type wounds had significantly higher integrin α6 expression at day 7 post-wounding compared with $Flii^{Tg/+}$ wounds (Figures 8b and 9b). $Flii^{+/-}$ wounds appeared to have delayed the expression of α6; however, its expression remained elevated for a long time and remained significantly increased compared with wildtype and $Flii^{Tg/+}$ at day 21, when the wounds were completely re-epithelialized (Figure 9b).

Integrin β4 is expressed on cell surfaces as a heterodimeric complex with integrin α6, forming a functional laminin integrin receptor α6β4, which associates with CD151 and plectin to stabilize the hemidesmosome adhesion complex and plays an important role in mediating cellular migration (Watt, 2002). Expression of integrin β4 was also altered in response to wounding with different levels of *Flii* gene expression. In unwounded skin, integrin β4 is mainly expressed on basal keratinocytes and upon wounding the expression increases and eventually upon hemidesmosome disassembly integrin β4 relocates to suprabasal keratinocytes of the migrating tongue and lamellipodial structures mediating cellular migration (Watt, 2002; Santoro and Gaudino, 2005). This pattern of increasing the integrin β4 expression was seen in response to wounding in $Flii^{+/-}$, wild-type, and $Flii^{Tg/+}$ wounds in both the epidermis (Figures 8b and 9c) and wound matrix (data not shown) although temporal differences were observed. Integrin β4 expression increased in wild-type wounds at day 3, peaking at day 7 before returning to basal levels by day 14 post-wounding. Interestingly, in both $Flii^{+/-}$ and $Flii^{Tg/+}$ wounds integrin β4 expression peaked earlier at day 3, decreased by day 7 and returned to basal levels by day 14 post-wounding (Figure 9c). Integrin β4 expression was significantly higher in $Flii^{+/-}$ and $Flii^{Tg/+}$ wounds at day 3

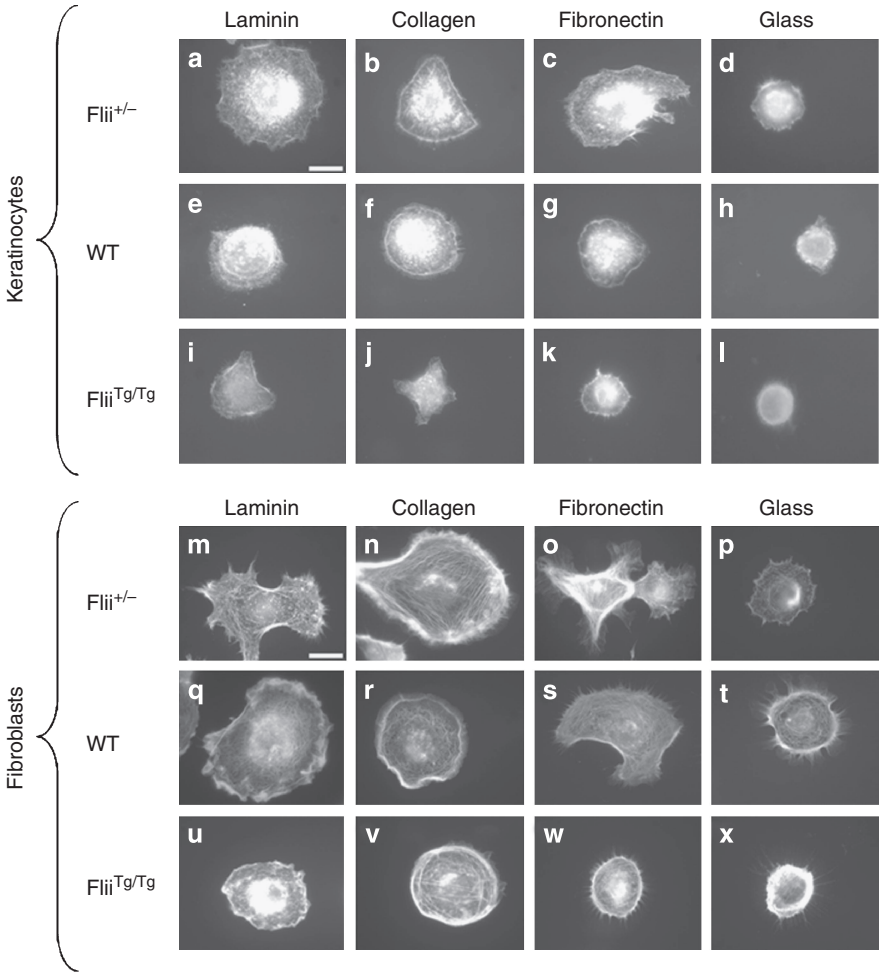


**Figure 4. Flii affects cellular spreading on different extracellular matrix substrates.** Keratinocyte (**a–l**) and fibroblast (**m–x**) spreading on laminin, collagen I, fibronectin and glass was examined by staining cells with phalloidin-FITC. Representative images of cell spreading on different substrates are shown in **a–x**. Magnification ×100. Scale bar in a and $m = 10\,\mu m$ and refers to all images.

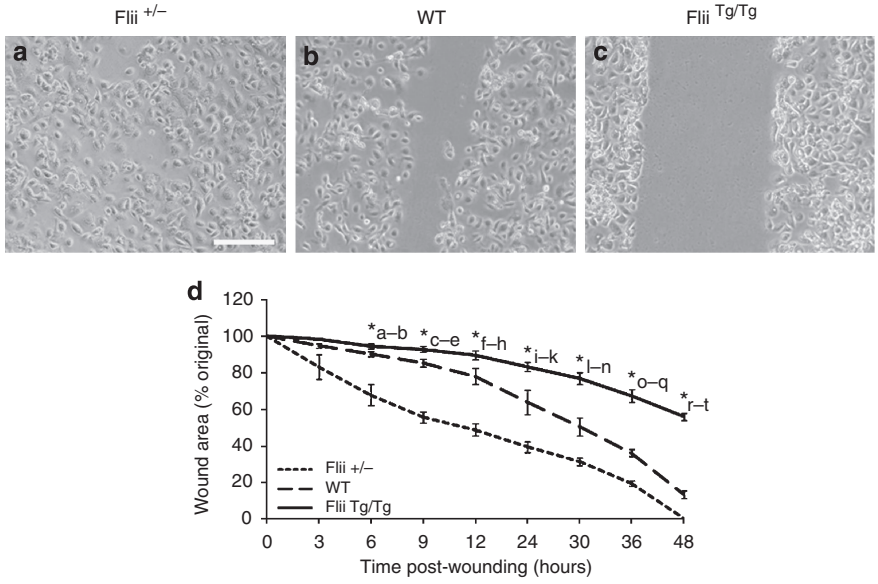


**Figure 5. Flii regulates keratinocyte cell migration.** (**a–c**) Representative images of scratch wound areas in $Flii^{+/-}$, wild-type, and $Flii^{Tg/Tg}$ keratinocytes 48 hours post-wounding. (**d**) Graph showing change in wound area over 48 hours of keratinocyte migration. $Flii^{Tg/Tg}$ and wild-type keratinocytes have significantly decreased wound area compared to $Flii^{+/-}$ counterparts (*a–t) respectively. Results represent mean and standard error of mean, $n = 6$, $^*P < 0/05$. Scale bar in a = 100 μm and refers to all images.

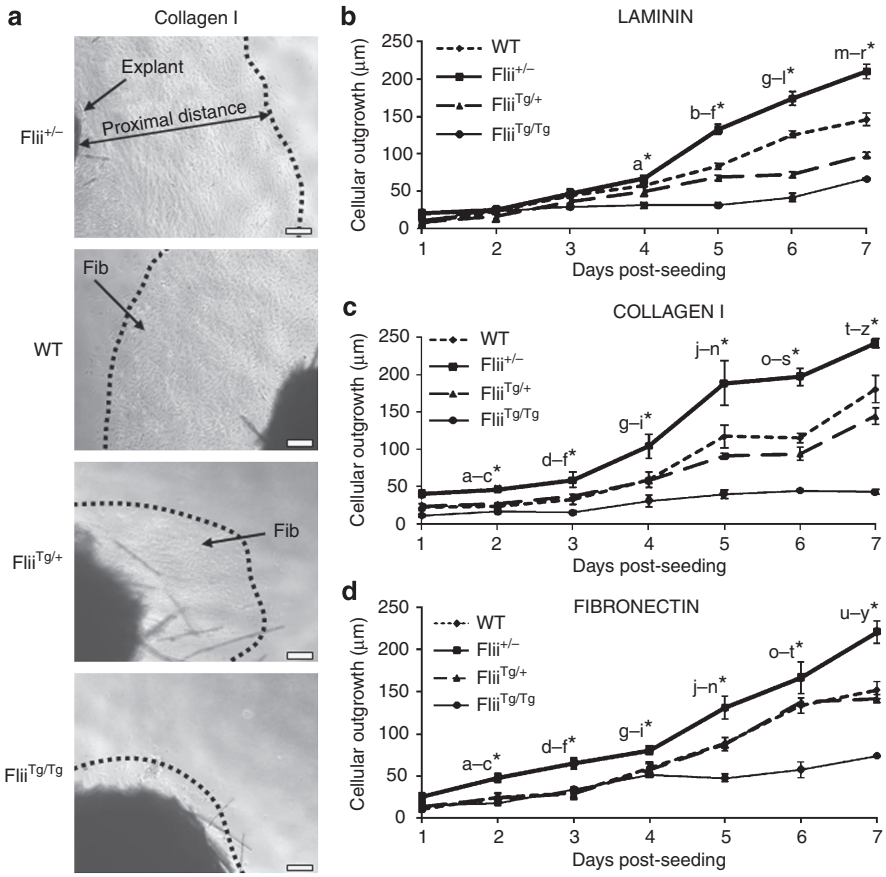


**Figure 6. Differential effects of Flii on fibroblast outgrowth from skin explants.** Here, 2 mm punch biopsies from *Flii*$^{+/-}$, WT, *Flii*$^{Tg/+}$, and *Flii*$^{Tg/Tg}$ were allowed to adhere to collagen I, laminin, and fibronectin-coated coverslips prior to culturing over 7 days. Images were taken daily and cellular outgrowth measured as proximal distance. (**a**) Representative images of cellular outgrowth on collagen I taken at day 6 post planting. Fib = fibroblasts. Scale bar = 100 μm. (**b**) *Flii*$^{+/-}$ cells have significantly increased outgrowth on laminin compared to *Flii*$^{Tg/Tg}$ fibroblasts from day 4 post-seeding, and compared to both WT and *Flii*$^{+/-}$ cells from day 5 post-seeding. (*a–r respectively). (**c**) Cellular outgrowth on collagen I shows a similar pattern to laminin, where *Flii*$^{+/-}$ cells have increased outgrowth compared to WT, *Flii*$^{Tg/+}$, and *Flii*$^{Tg/Tg}$ fibroblasts (*a–z), respectively. (**d**) Cellular outgrowth on fibronectin is similar to those on laminin and collagen I, except no significant difference is observed between WT and *Flii*$^{Tg/+}$ fibroblasts outgrowth (*a–y, respectively). Figure represents means and standard error of means. *$P<0.05$.

post-wounding compared with wild-type counterparts (Figure 8b). At day 7 post-wounding, integrin β4 expression was significantly decreased in *Flii*$^{+/-}$ and *Flii*$^{Tg/+}$ wounds compared to wild-type counterparts and *Flii*$^{Tg/+}$ wounds had significantly higher integrin β4 compared with *Flii*$^{+/-}$ wounds. By day 14 and 21 post-wounding integrin β4 levels had returned to basal levels when new adhesion sites were already formed (Figure 9c)

### Flii co-localizes with focal contact proteins and may modulate integrin-dependent signaling

To gain a mechanistic insight into the role of Flii in the hemidesmosome structure and function, keratinocytes (HaCaTs) were used to investigate possible Flii-binding partners. A number of potential binding candidates were targeted including integrin chains β1, β4, tetraspanin CD151, and focal contact proteins know to associate directly with integrin β1 and form cytoskeletal complexes involved in integrin-dependent signaling pathways including; talin, α-actinin, vinculin, and paxillin. Immunoprecipitates and cell lysates from wounded keratinocytes were analyzed using western blotting. Flii was not observed to co-immunoprecipitate with integrin chains β1, β4, and CD151 (Figure 10a). Dual immunofluorescence also showed no direct binding of Flii with these proteins (data not shown). Flii did however immunoprecipitate with talin, paxillin, and vinculin, but not α-actinin (Figure 10b) and this binding was confirmed using dual-labeled immunofluorescence (Figure 10c).

## DISCUSSION

Cellular migration and adhesion in response to wounding, requires complex re-organization of the actin cytoskeleton in a spatially and temporally coordinated manner. These processes are controlled by both extracellular and intracellular processes, including control at the level of actin cytoskeletal remodelling and at sites where cells adhere to the extracellular matrix. Efficient hemidesmosome disassembly upon wounding and quick formation of new stable adhesion sites are important events in wound repair, allowing cellular migration over the provisional wound bed and strong adhesion at the dermal–epidermal junction (Jones *et al.*, 1998). Recent advances in integrin receptor structure have

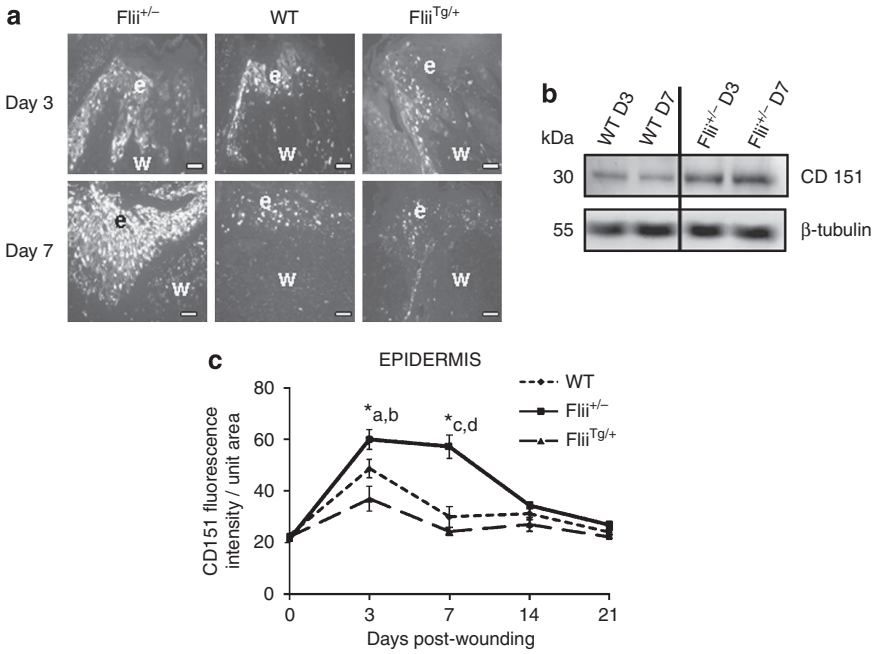


**Figure 7. CD151 expression is increased in *Flii*-deficient mice during wound repair.** (**a**) CD151 expression detected as a white fluorescence in the epidermis and dermis of wounded Flii$^{+/-}$, WT, and *Flii*$^{Tg/+}$ skin at day 3 and 7 post-wounding. Epidermis = e. Wound matrix = w. Magnification ×40, scale bar = 100 μm. (**b**) Western Blot analysis of CD151 and β-tubulin (control) in protein extracted from WT and *Flii*$^{+/-}$ skin at day 3 and 7 post-wounding. (**c**) Both *WT* (*a) and *Flii*$^{+/-}$ (*b) wounds have significantly increased CD151 expression in epidermis at day 3 post-wounding when compared to *Flii*$^{Tg/+}$ wounds. *Flii*$^{+/-}$ wounds also have significantly increased CD151 expression compared to *WT* (*c) and *Flii*$^{Tg/+}$ (*d) wounds at day 7 post-wounding. Figure represents means and standard error of means. $n = 6$ per group per time point. *$P < 0.05$.

revealed an increasing number of integrin-binding cytoskeletal proteins involved in integrin-dependent adhesion-signaling pathways (Arnaout *et al.*, 2007). The current study now shows that Flii plays an important role in the formation and maintenance of stable adhesion sites of the basement membrane at the dermal–epidermal junction and may be involved in integrin-signaling pathways, mediating keratinocyte and fibroblast migration, adhesion, and spreading.

*Flii* overexpressing mouse skin have significantly decreased tensile strength and fewer numbers of hemidesmosomes than wild-type and *Flii*$^{+/-}$ mice. Under normal conditions, hemidesmosomes have a triangular cytoplasmic inner plaque, a sub-basal dense plate just below and external to the basal membrane and thin extracellular anchoring filaments which extend from the plate into the basement membrane (Jaunzems *et al.*, 1997). Using electron transmission microscopy, we observed shorter hemidesmosomes, with reduced inner plaque and a reduced percentage of hemidesmosomes with sub-basal dense plates in *Flii*$^{Tg/+}$ and *Flii*$^{Tg/Tg}$ mice skin. A decreased number of hemidesmosomes and shorter hemidesmosome length would result in decreased hemidesmosome contact along the dermal–epidermal junction aspect of basal keratinocytes leading to weakened hemidesmosome to tonofilament interaction, delayed formation of new adhesion sites, and impaired re-epithelialization, as was observed in these mice (Cowin *et al.*, 2007). In agreement with altered hemidesmosome structure, *Flii*$^{Tg/Tg}$ keratinocytes and fibroblasts showed significantly decreased adhesion and spreading on laminin, fibronectin and collagen I compared with wild-type counterparts. In addition, both *Flii*$^{+/-}$ keratinocytes and fibroblasts had significantly improved adhesion and spreading on laminin and collagen I extracellular matrix substrates. Decreased *Flii* gene expression also increased the rate of keratinocyte migration and improved cellular outgrowth from *Flii*$^{+/-}$ skin explants on laminin, collagen I and fibronectin substrates indicating the important role of Flii in regulating cellular adhesion and migration.

The tetraspanin CD151, an integral part of hemidesmosomes, is expressed in both keratinocytes and fibroblasts and, although its effects on migration depend on both cell type and extracellular matrix substrates, studies have shown that CD151 activity enhances integrin cell adhesion structures by providing hemidesmosome and intercellular junction stability (Chometon *et al.*, 2006). We have previously shown that CD151 is involved in wound re-epithelialization, affecting both cellular adhesion and migration, and that CD151 null mice exhibit retarded epidermal and dermal contraction (Cowin *et al.*, 2006; Geary *et al.*, 2008). CD151 regulates adhesion by being an integral part of hemidesmosomes, where it associates with integrin α3β1 and laminin-5 to form pre-hemidesmosomal integrin clusters serving as a nucleation site for the assembly of stable hemidesmosomes by the integrin α6β4, contributing to the efficacy of hemidesmosome formation (Litjens *et al.*, 2006). Recent studies indicate that CD151 catalyzes the cell migratory activity by regulating the glycosylation of integrin α3β1 (Baldwin *et al.*, 2008) and indirectly associates with collagen and fibronectin integrin

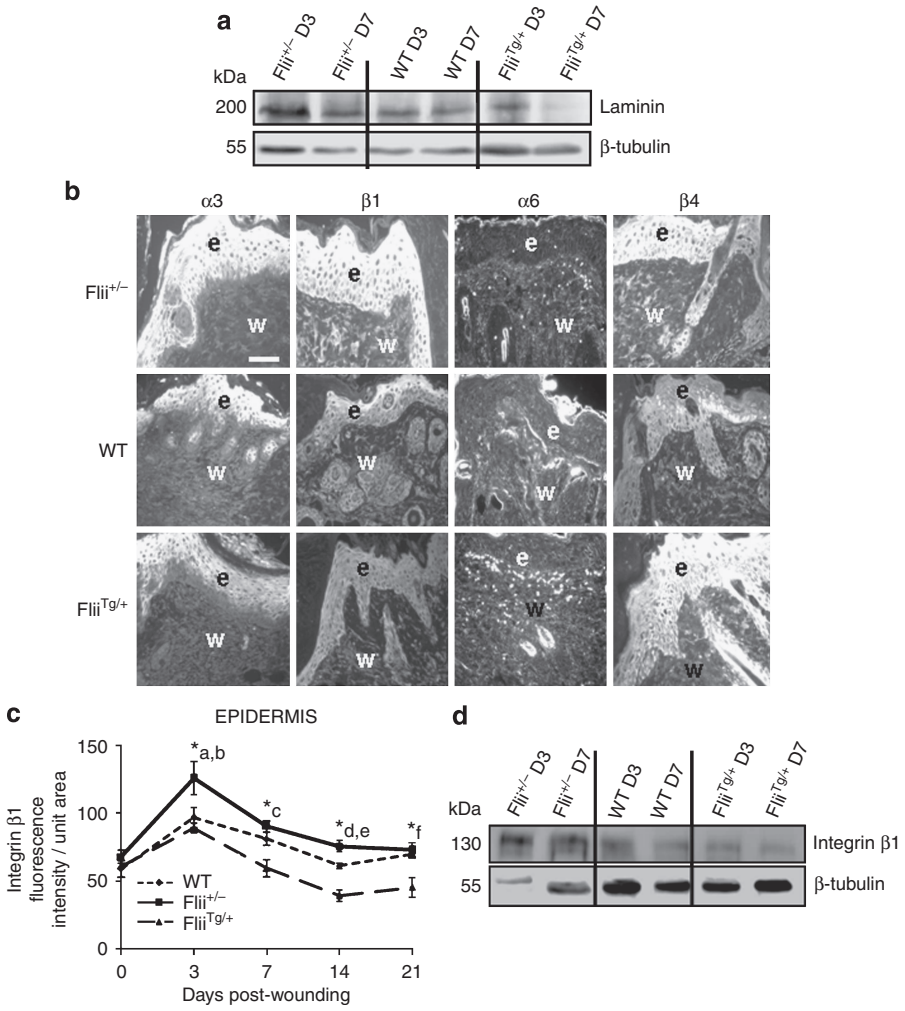


**Figure 8. Manipulation of Flii results in altered expression of laminin and laminin-binding integrin α3, β1, α6, and β4 subunits.** (**a**) Western blot analysis of laminin and β-tubulin (control) in protein extracted from *Flii*$^{+/-}$, wild-type and *Flii*$^{Tg/Tg}$ skin at day 3 and 7 post-wounding. *Flii*$^{+/-}$ have increased laminin expression compared to wild-type and *Flii* overexpressing mice. (**b**) α3, β1, α6, and β4 integrin expression detected as white fluorescence in the epidermis and dermis of wounded skin at day 3 post-wounding. Epidermis = e. Wound matrix = w. Scale bar in (**a**) refers to all images = 100 μm. (**c**) Graph showing quantitative analysis of integrin β1 expression in the epidermis of *Flii*$^{+/-}$, WT, and *Flii*$^{Tg/+}$ wounds. *Flii*$^{+/-}$ wounds have significantly increased β1 integrin expression compared to WT wounds at day 3(*a) and 14 (*d) post-wounding and compared to *Flii*$^{Tg/+}$ wounds at day 3(*b), 7 (*c), 14 (*e), and 21 (*f) post-wounding. (**d**) Western blot analysis of β1 integrin in protein extracted from *Flii*$^{+/-}$, WT, and *Flii*$^{Tg/+}$ skin at day 3 and 7 post-wounding. Figure represents means and standard error of means. $n = 6$ per group per time point. *$P < 0.05$.

receptors, α2β1 α5β1 respectively, to influence fibroblast-mediated dermal contraction (Sincock *et al.*, 1999; Liu *et al.*, 2007). *Flii*$^{+/-}$ mice have significantly increased CD151 and laminin protein expression in response to wounding which may contribute to improved cellular migration and wound contraction through association of this tetraspanin with different integrin receptors and laminin extracellular matrix substrate. Furthermore, *Flii*$^{Tg/+}$ mice wounds had significantly decreased CD151 expression compared with wild-type counterparts which may have affected the observed irregular formation of poorly defined hemidesmosomes by decreasing the number of pre-hemidesmosomal integrin clusters and delayed re-epithelialization and wound contraction observed in these mice (Cowin *et al.*, 2007).

The expression levels of laminin-binding integrin chains, α3, β1, α6, β4 in wounded *Flii*$^{+/-}$, wild-type and *Flii*$^{Tg/+}$ skin were examined as these are the predominant binding partners of CD151 in epithelial tissue. Integrin receptor α3β1 binds to unprocessed laminin and stimulates migration of the first row of keratinocytes over the provisional wound matrix which then secrete more laminin for subsequent cells to migrate and cover the wound (Nguyen *et al.*, 2000). Although we observed elevated α3 expression in unwounded skin of *Flii*$^{+/-}$ versus wild-type versus *Flii*$^{Tg/+}$ mice all subsequent effects of wound healing were in proportion to these basal levels. In contrast, reduced *Flii* gene expression resulted in increased integrin β1 protein levels whereas overexpression of *Flii* led to decreased levels of integrin β1, which may have resulted in a decreased expression of different integrin receptors or their affinity for extracellular matrix ligands and could adversely affect cellular migration and fibroblast wound contraction. Integrin β1 chain expression is vital

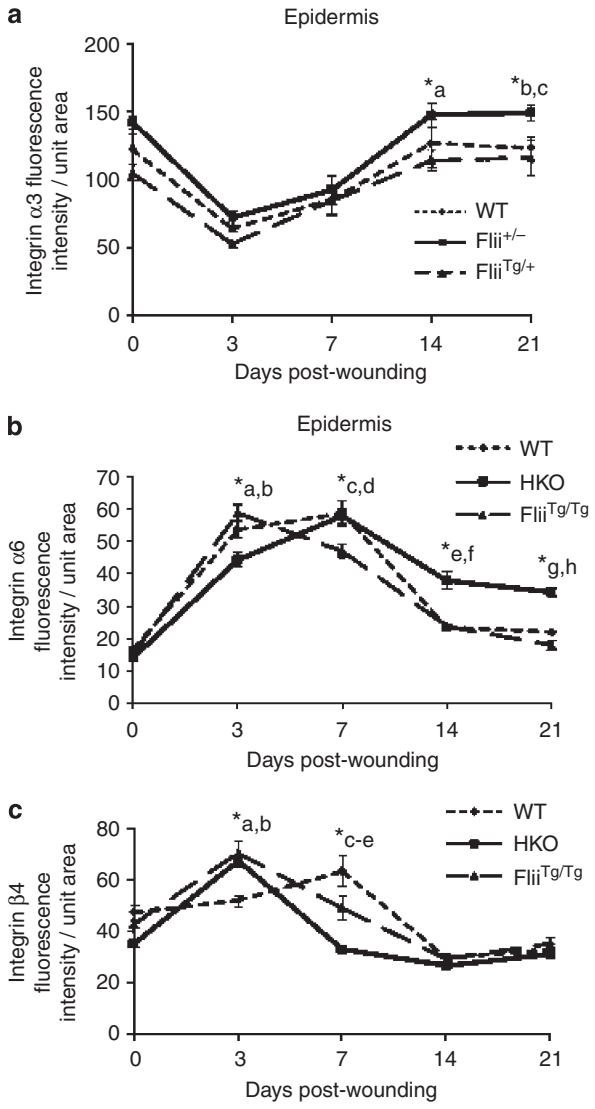


**Figure 9. Graphical representation of α3, α6, and β4 integrin optical density in *Flii*$^{+/-}$, WT, and *Flii*$^{Tg/+}$ wounds.** (**a**) *Flii*$^{+/-}$ wounds have significantly increased α3 integrin expression compared to *Flii*$^{Tg/+}$ (*a) wounds at day 14 post-wounding and compared to both WT (*b) and *Flii*$^{Tg/+}$ (*c) wounds at day 21 post-wounding. (**b**) *Flii*$^{+/-}$ wounds have significantly decreased α6 integrin expression compared to *Flii*$^{Tg/+}$ (*a) and WT (*b) wounds at day 3 post-wounding. At day 7 post-wounding both WT (*c) and *Flii*$^{+/-}$ (*d) wounds have significantly increased α6 integrin expression compared to *Flii*$^{Tg/+}$ wounds. *Flii*$^{+/-}$ wounds have significantly higher α6 integrin expression compared to WT and *Flii*$^{Tg/+}$ mice wounds at day 14 (*e, f) and 21 (*g, h) post-wounding, respectively. (**c**) In the epidermis, both *Flii*$^{+/-}$ (*a) and *Flii*$^{Tg/+}$ (*b) wounds have significantly higher β4 integrin expression at day 3 post-wounding when compared to WT counterparts. At day 7 post-wounding, WT wounds have significantly higher expression of β4 integrin compared to *Flii*$^{Tg/+}$ (*c) wounds whereas *Flii*$^{+/-}$ wounds have significantly decreased β4 integrin expression compared to both WT(*d) and *Flii*$^{Tg/+}$ (*e) wounds. Figure represents means and standard error of means. $n=6$ per group per time point. *$P<0.05$.

during wound repair as it associates with different integrin α chains to form laminin, collagen, and fibronectin receptors and its loss or decrease results in impaired cell migration, decreased cell proliferation and aberrant deposition of extracellular matrix proteins namely, laminin and collagen (Brakebusch and Fassler, 2005). Integrin β1 also directly links to the actin cytoskeleton and provides a degree of stabilization, which is tightly regulated to provide optimal traction forces required for cellular migration (Chometon *et al.*, 2006).

Mouse wounds displayed an altered expression of integrin α6 and β4 chains in response to different *Flii* gene levels. These two integrin chains combine to form a functional α6β4 integrin receptor, which binds to processed laminin and stabilizes the cell–substrate interactions and induces formation of hemidesmosomes once the wound is re-epithelialized (Jones *et al.*, 1998). Integrin α6 staining was observed in basal keratinocytes and fibroblasts within the wound matrix. Interestingly, at day 3 post-wounding wild-type and *Flii*$^{Tg/+}$ wounds had significantly increased integrin α6 expression compared with *Flii*$^{+/-}$ wounds suggesting that *Flii*$^{+/-}$ mice may have weaker cell–substrate interactions. At day 7 post-wounding, once the wound was re-epithelialized, *Flii*$^{Tg/+}$ wounds had a significantly reduced expression of α6, which may lead to impairment in the formation of new hemidesmosomes. In contrast to integrin α6 chain expression, we found that both *Flii*$^{+/-}$ and *Flii*$^{Tg/+}$ wounds displayed an earlier, increased response in integrin β4 chain expression upon wounding compared with wild-type wounds, where integrin β4 chain expression peaks at day 7 post-wounding. We observed a redistribution of integrin β4 chain to the basolateral/suprabasal surface in agreement with studies in α6 knockout mice, where integrin β4 chain is not concentrated in basal keratinocytes suggesting that polarized expression of integrin β4 is dependent upon presence of an integrin α6 chain (Georges-Labouesse *et al.*, 1996; Manohar *et al.*, 2004). The long cytoplasmic chain of integrin β4 recruits a number of signaling molecules involved in cellular proliferation (Mainiero *et al.*, 1997; Raymond *et al.*, 2005) and increased expression of integrin β4 in the absence of integrin α6 chain suggest an involvement of integrin β4 in signaling cascades independent of its adhesive function. However, contradictory responses in integrin β4 expression to *Flii* gene expression suggest that integrin β4 chain expression may not be directly affected by *Flii*.

Our results indicate a role for Flii in cellular migration and proliferation however the exact mechanisms by which Flii affects wound healing are yet to be elucidated. Although Flii is secreted in response to wounding (Cowin *et al.*, 2007) its main roles include intracellular actin remodelling and nuclear transcription implicating the role of Flii in different signaling pathways. Flii is associated with actin arcs and membrane ruffles where it co-localizes with GTP-binding proteins that have central roles in regulating cytoskeletal re-organization (Kaibuchi *et al.*, 1999). Focal adhesions are important sites of signal transduction, where numerous proteins are involved in converging the integrin signals to the downstream effectors. Indeed, a number of actin-binding cytoskeletal proteins, including talin and α-actinin, have been shown to be present at the epidermal–dermal interface and interact directly with the integrin β1 cytoplasmic domain of the hemidesmosome protein complex forming a cytoskeletal complex and modulating different signal transduction pathways and cellular behavior (Gonzalez *et al* 2001; Zhang

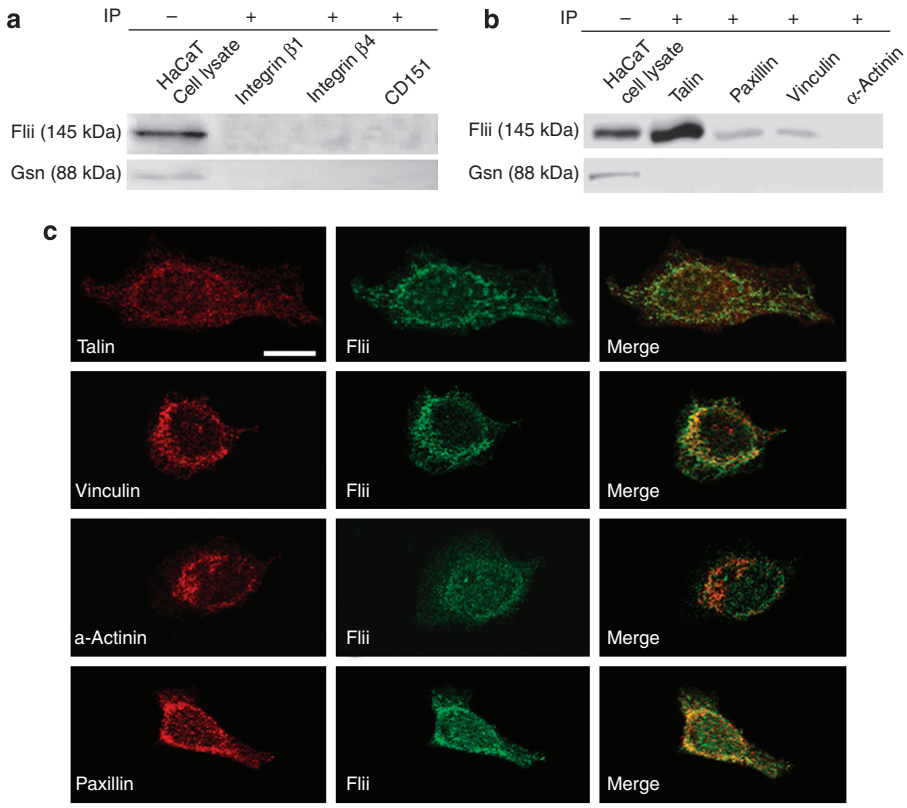


**Figure 10. Flii co-localization with integrin-binding proteins involved in adhesion-dependent signaling pathways.** (**a**) Anti-integrin β1, β4, and tetraspanin CD151 immunoprecipitates (IP) were prepared from confluent HaCaTs keratinocytes and immunoblotted with Flii or Gelsolin (positive control) antibodies. No co-localization was observed with Flii and integrins β1, β4, or tetraspanin CD151 and specific bands were only observed in HaCaTs cell lysate controls. (**b**) Anti-talin, paxillin, vinculin, and α-actinin immunoprecipitates (IP) were prepared from confluent HaCaTs keratinocytes and immunoblotted with Flii and Gelsolin (positive control) antibodies. Flii colocalized with all actin-binding cytoskeletal proteins except α-actinin. Data are representative of three independent experiments. (**c**) Representative confocal images of dual immunofluorescence on HaCaTs keratinocytes illustrating Flii (green) and different actin-binding protein (red) staining. Merged images show Flii co-localization with talin, vinculin, and paxillin but not α-actinin. Magnification × 100. Scale bar = 10 μm and refers to all images. Data are representative of three independent experiments.

*et al.*, 2008). Here, we show that Flii does not bind directly to integrin β1, β4, and tetraspanin CD151 during wounding; however, it does interact with talin, paxillin, and vinculin actin-binding proteins, which form the cytoskeletal complex directly linking the integrin receptors to the actin cytoskeleton (Critchley *et al.*, 1999). Paxillin is known to bind to many proteins effecting the changes in the organization of the actin cytoskeleton required for cell motility and wound repair. Our results therefore suggest that Flii may be directly involved in integrin-mediated adhesion by binding to associated cytoskeletal complexes, hence suppressing the function of the activated ligand-bound integrin receptors and mediating integrin-dependent signaling pathways. Flii overexpression may result in decreased integrin clustering, altered hemidesmosome adhesion complex and inhibition of the delicate mechanical connection between ligand-bound integrin receptors and the actin cytoskeleton required to impel different adhesion-dependent signaling pathways. Consequently, the effect of Flii on different adhesion-signaling pathways may result in altered expression levels of integrin receptors, laminin protein, and tetraspanin CD151 as observed in the impaired healing response of *Flii* overexpressing mouse wounds. In summary, Flii is a potentially important regulator of wound healing through processes involving hemidesmosome formation and integrin-mediated cellular adhesion and migration. Manipulation of this protein may lead to potential new advances in improving wound repair.

## MATERIALS AND METHODS

### Reagents and antibodies

Rabbit anti-CD151 (sc-18753) was obtained from Santa Cruz (Santa Cruz, CA) and is an antibody raised against a peptide mapping near the amino terminus of human CD151. Integrin α6 (sc-6596) raised against epitopes corresponding to an amino acid sequence mapping at the carboxy terminus of the precursor form of integrin α6 of human origin was obtained from Santa Cruz. Integrin α3 (sc-28665), integrin β1 (sc-8978), and integrin β4 (sc-9090) were obtained from Santa Cruz and are rabbit polyclonal antibodies raised against amino acids mapping within an extracellular domain of integrin α3, integrin β1, and integrin β4 of human origin, respectively. Antibodies specific against human α-actinin (05-384), paxillin (05-417), talin (05-385), and vinculin (05-386) were purchased from Upstate Biotechnology, USA. Paxillin antibody was raised against a GST

fusion protein containing the full-length human paxillin. Rabbit anti-Flightless I antibody is raised against amino acids 1–300 mapping at the N terminus of Flightless I of human origin (Santa-Cruz) whereas Gelsolin was sourced from BD Biosciences, North Ryde NSW. Collagen type I (C-8919) from calf skin, Laminin (L-6274) from human placenta and Fibronectin (F-1141) from bovine plasma, were all purchased from Sigma-Aldrich Pty. Ltd., Sydney, Australia. β-tubulin antibody was obtained from Sigma-Aldrich.

### Animal studies

All experiments were approved by the Adelaide Women's and Children's Hospital Animal Care and Ethics Committee and the Australian National University Animal Ethics Committee following the Australian Code of Practice for the Care and the Use of Animals for Scientific Purposes. Studies were performed using mice with the BALB/c background. *Flii* homozygous mutant mice are embryonic lethal (Campbell *et al.*, 2002). *Flii*-deficient heterozygous null mice ($Flii^{+/-}$) and mice carrying the complete human *Flii* gene on a cosmid transgene were as described previously (Campbell *et al.*, 2002, Cowin *et al.*, 2007). Heterozygous transgenic mice $Flii^{Tg/+}$ were made by crossing $Flii^{+/+}$ with cosmid transgene $Flii^{+/-}$. These transgenic mice were intercrossed to obtain animals homozygous for the transgene ($Flii^{Tg/Tg}$).

### Murine surgical techniques

$Flii^{+/-}$, wild-type, $Flii^{Tg/+}$, and $Flii^{Tg/Tg}$ female 12-week-old mice, were anaesthetized using gaseous isofluorane, 5% induction, 2% maintenance and wounded using the same protocol previously described (Cowin *et al.*, 2006; Kopecki and Cowin, 2008). Briefly, two equidistant, 1 cm full thickness incisions were made through the skin and panniculus carnosus using fine scissors on the flanks of the animals extending 3.5–4.5 cm from the base of the skull, 1 cm either side of the spinal column. The wounds were left to heal by secondary intention (that is, the wound edges were not closed by sutures). At 3, 7, 14, and 21 days post-wounding, mice were euthanized using $CO_2$ asphyxiation and cervical dislocation prior to harvesting of the wounds. Both left and right wounds were collected from each mouse and bisected. One half was fixed in 10% buffered formalin and the other half for biochemical analysis was micro-dissected to remove any contaminating normal, unwounded skin and snap frozen in liquid nitrogen for protein extraction and western blot analysis. Unwounded skin was collected from each mouse group.

### Hemidesmosome analysis

Two millimeters punch biopsies (Acupunch, ACUDERM) excised from 12-week-old female $Flii^{+/-}$, wild-type, $Flii^{Tg/+}$ and $Flii^{Tg/Tg}$ mouse skin were fixed overnight in 4% paraformaldehyde/1.25% glutaraldehyde/4% sucrose in phosphate-buffered saline (PBS), pH 7.2. Tissue punch biopsies were subsequently washed for 10 minutes in two changes of 4% sucrose/PBS followed by post-fixation in aqueous 2% osmium tetroxide for 1 hour on a rotator. After washing, specimens were dehydrated in a graded series of ethanol (70–100%) followed by further dehydration in propylene oxide for 30 minutes. Tissue samples were resin infiltrated with 1:1 propylene oxide/resin solution overnight followed by an 8-hour incubation in three changes of 100% epoxy resin. Tissue samples were then embedded in fresh resin (Procure Araldite embedding kit) and polymerized at 70°C overnight. For orientation purposes, semi-thin (1 μm thick) survey sections were cut on a Reichert Ultracut S ultramicrotome and stained with 1% toluidine blue in 1% borax. Ultra thin sections were cut and mounted on 100 mesh hexagonal copper grids (Gilder Grids, Grantham, UK). Sections were stained with 2% uranyl acetate for 10 minutes followed by 1% lead citrate for 7 minutes and examined with a Phillips CM100 transmission electron microscope operated at an accelerating voltage of 80 kV.

Electron micrographs were taken of two different skin samples of unwounded $Flii^{+/-}$, wild-type, $Flii^{Tg/+}$ and $Flii^{Tg/Tg}$ at different magnifications ranging from $\times 7{,}900$ to $\times 92{,}000$ with random selection of sections. Tissue skin architecture and structure was observed particularly focusing on regions of dermal–epidermal junction and a number of different parameters were analyzed using Image Pro-Plus 5.1 program (MediaCybernetics Inc.). These included: number of hemidesmosomes/basement membrane length (μm), number of hemidesmosomes with sub-basal dense plates and their percentage in relation to the total number of hemidesmosomes counted, average lamina lucida and lamina densa thickness of basal lamina, and average hemidesmosome length ($n = 150$ hemidesmosomes). Density of tonofilaments and anchoring fibrils, density of collagen fibers, structural features of hemidesmosomes and desmosomes as well as other structural features of both dermis and epidermis were assessed as previously described in Jaunzems *et al.* (1997).

### Primary keratinocyte isolation

Primary murine keratinocytes were isolated and cultured following protocols described by Redvers and Kaur (2004). Briefly, tails were collected from euthanized 12-week-old BALB/c Flii +/−, wild-type, and Flii Tg/Tg mice and skin peeled from the underlying tail cartilage and incubated in Dispase (8 mg ml$^{-1}$) (Roche, Australia) overnight 4°C to dissolve the dermal–epidermal junction. Using a dissecting microscope, epidermis was peeled in the direction of the hair follicles and transferred to the pre-warmed trypsin-EDTA (Sigma-Aldrich) and placed on a magnetic stirring plate at 500 r.p.m. for 4 minutes. The reaction was then quenched by placing the solution on ice and adding an equal volume of the trypsin inhibitor (Sigma-Aldrich, Sydney, Australia). Epidermal slurry was passed through 70 μm and 40 μm cell strainers (BD Biosciences) and cells centrifuged at 400 g for 5 minutes at 4°C. The cell pellet was resuspended and cells were cultured on 20 μg ml$^{-1}$ Collagen IV (20 μm) coated plates in PCT Epidermal Keratinocyte-Defined Medium Cnt-07 (Millipore, Australia), 5% Penicillin Streptomycin, 5% Fungizone (Sigma-Aldrich) at 37°C, 5% $CO_2$. Passages 2–5 were used in all experiments.

### Primary fibroblast isolation

Hair was shaved from the dorsal flank of euthanized 12-week-old female $Flii^{+/-}$, wild-type, $Flii^{Tg/+}$ and $Flii^{Tg/Tg}$ mice and skin excised and collected in ice-cold Ham's Nutrient Mixture F12 (SAFC Biosciences, Lenexa, KS), 5% Penicillin Streptomycin, 5% Fungizone (Sigma-Aldrich). Skin was cut into small $5 \times 5$ mm pieces with sterile scissors in sterile conditions and placed dermal side down into 12-well plates. Explants were allowed to partially dry and fix to the bottom of the well before 2 ml Dulbecco's modified Eagle's medium (DMEM), 20% fetal calf serum (FCS), 5% Penicillin Streptomycin, 5% Fungizone was added and cultured in 37°C, 5%

$CO_2$, replacing media after 24 hours and then every 2 days. Once fibroblasts migrated out from the explant the skin was removed and cells cultured as normal in 10% FCS/DMEM, 5% Penicillin Streptomycin. Passages 2–5 were used in all experiments.

### Fibroblast and keratinocyte hexosaminidase adhesion assay

Flii +/−, wild-type and Flii Tg/Tg primary keratinocytes and fibroblasts were grown to 60% confluence in PCT epidermal keratinocyte-defined medium Cnt-07 (Millipore), 5% Penicillin Streptomycin, 5% Fungizone (Sigma-Aldrich) and 10% FCS/DMEM, 5% Penicillin Streptomycin, 5% Fungizone (Sigma-Aldrich), respectively. Primary fibroblasts were serum-starved overnight in 0.5% FCS to synchronize the cells to the G1 phase of the cell cycle. Fibroblasts and keratinocytes were trypsinized and seeded at $5 \times 10^4$ cells per ml onto pre-coated 96-well plates with 10 μg ml$^{-1}$ Fibronectin, 6 μg ml$^{-1}$ Laminin, or 10 μg ml$^{-1}$ Collagen I (Sigma-Aldrich). Following the protocol described in May *et al*. (2001) the wells were blocked with 0.5 mg ml$^{-1}$ BSA, prior to cell seeding. To account for non-specific adhesion some wells were coated with BSA only and wells with no cells were set up as controls. Keratinocytes and fibroblasts were allowed to adhere to the extracellular matrix by incubation at 37°C for 6 hours and 90 minutes, respectively. Following the incubation, the non-adhered cells were gently washed with PBS-ABC, and 60 μl of the enzyme substrate PNAG (Sigma-Aldrich) was added to each well and incubated with the attached cells for an additional hour in the 37°C incubator. Enzyme activity was then blocked and color reaction was developed by adding 90 μl of 50 mM glycine buffer. The absorbance was measured at 405 nm on an ELISA plate reader. Percentage of cell adhesion to different extracellular matrix substrate was calculated by using the absorbance values and cell adhesion was expressed as a percentage of adhesion of wild-type cells.

### Scratch assay

Primary keratinocytes isolated from Flii +/−, wild-type, and Flii Tg/Tg mice skin were grown to confluence in PCT epidermal keratinocyte-defined medium Cnt-07 (Millipore), 5% Penicillin Streptomycin, 5% Fungizone (Sigma-Aldrich) at 37°C, 5% $CO_2$ on glass coverslips and scratched with a P200 pipette tip, producing equal size wounds of 2 mm × 1 cm. The cells were photographed at 0, 3, 6, 9, 12, 24, 30, 36, and 48 hours post-wounding and wound area measured using the Image Pro-Plus program (MediaCybernetics Inc.). The rate of keratinocyte migration and wound closure was quantified as a percentage of the initial wound area.

### Cell spreading

Keratinocytes and fibroblast spreading on coverslips coated with different extracellular matrix substrates including: 10 μg ml$^{-1}$ Fibronectin, 6 μg ml$^{-1}$ Laminin or 10 μg ml$^{-1}$ Collagen I (Sigma-Aldrich) was assessed by seeding keratinocytes in PCT epidermal keratinocyte-defined medium Cnt-07 (Millipore), 5% Penicillin Streptomycin, 5% Fungizone (Sigma-Aldrich) and fibroblasts in 10% FCS/DMEM, 5% Penicillin Streptomycin, 5% Fungizone (Sigma-Aldrich) at 37°C, 5% $CO_2$, acetone-fixing cells at 6 hours and 90 minutes post-seeding respectively. Following blocking in 3% normal horse serum, phalloidin-FITC (Sigma-Aldrich) was added at 1:200 for 1 hour staining in the dark. Representative images of cell spreading on different extracellular matrix substrates and glass control were taken using AnalySIS software package (Soft Imaging System GmbH, Muster, Germany), illustrating filamentous actin fibers. All control sections had negligible immunofluorescence.

### Skin explant outgrowth assay

2 mm punch biopsies (Acupunch, ACUDERM) excised from *Flii*$^{+/-}$, wild-type, *Flii*$^{Tg/+}$, and *Flii*$^{Tg/Tg}$ skin were collected in ice-cold Ham's Nutrient Mixture F12 (SAFC Biosciences), 5% Penicillin Streptomycin, 5% Fungizone (Sigma-Aldrich). Four punch biopsies per well were fixed dermal side down onto glass coverslips (controls) or coverslips pre-coated with 10 μg ml$^{-1}$ Fibronectin, 6 μg ml$^{-1}$ Laminin or 10 μg ml$^{-1}$ Collagen I (Sigma-Aldrich Pty. Ltd., St Louis, MO). Skin explants were cultured in 2 ml 20% FCS/DMEM, 5% Penicillin Streptomycin, 5% Fungizone (Sigma-Aldrich) at 37°C, 5% $CO_2$, replacing media after 24 hours and then every 2 days. Representative photographs of cellular outgrowth from each explant were taken daily and proximal distance of cellular migration out from the dermis measured at 0–7 days post plating.

### Histology, immunohistochemistry, and image analysis

Histological sections (4 μm) from paraffin-embedded fixed wound tissue of *Flii*$^{+/-}$, wild-type, *Flii*$^{Tg/+}$, and *Flii*$^{Tg/Tg}$ were cut, stained with haematoxylin and eosin, and analyzed using light microscopy for structural differences. Dermal thickness was determined by measuring the distance between basement membrane and the panniculus carnosus using Image Pro-Plus 5.1 program (MediaCybernetics Inc.). Immunohistochemistry was also performed on paraffin-embedded fixed wound tissue following antigen retrieval according to the manufacturer's protocols (DAKO Corporation, Glostrup, Denmark). Following blocking in 3% normal horse serum, primary antibodies against α3, α6, β1, β4 were applied at 1:100 and CD151 at 1:200, and slides were incubated at 4°C overnight in a humidified chamber. Species-specific, biotinylated secondary antibodies were used and detection was by CY3-conjugated streptavidin (1:200) (Sigma-Aldrich, St Louis, MO). Fluorescence intensity per unit area was determined using AnalySIS software package (Soft Imaging System GmbH) and optical fluorescence analyzed in epidermis and dermis of the wounds, as previously described in Cowin *et al*. (2007). InSpeck Microscope Image Intensity Calibration Kits (Invitrogen, Carls bad CA) were used to define fluorescence intensity levels for constructing calibration curves and evaluating sample brightness. Negative controls included replacing primary antibodies with normal rabbit IgG, or normal mouse IgG. For verification of staining, non-specific binding was determined by omitting primary or secondary antibodies. All control sections had negligible immunofluorescence.

### Western blotting

Protein was extracted from *Flii*$^{+/-}$, wild-type, and *Flii*$^{Tg/+}$ mouse wounds using standard protein extraction protocols. Briefly, wound tissue was microdissected to remove normal, unwounded skin, chopped and placed in lysis buffer (50 mM Tris pH 7.5, 1 mM EDTA, 50 mM NaCl, 0.5% Triton X-100) containing protease inhibitor cocktail tablet (1 per 10 ml; Complete, Mini (Roche Products Pty Ltd, Dee Why, NSW, Australia)) and samples were homogenized briefly. Samples were centrifuged (16 000 × g, 10 minutes, at 4°C), with supernatants being transferred to fresh tubes and centrifuged for a further 10 minutes and the supernatants stored at −20°C. Sample

protein (10 μg) was run on 10% SDS-PAGE gels at 100V for 1 hour and then transferred to nitrocellulose by wet transfer (Bio-Rad Laboratories, Regents Park, NSW, Australia) using standard Towbins Buffer with 20% Methanol at 100V for 1 hour. Membranes were blocked in 15% milk-blocking buffer for 10 minutes and primary antibodies added in PBS containing 5% skimmed milk powder, 0.3% Tween. Appropriate species-specific secondary horse radish peroxidase-conjugated antibodies were added for a further 1 hour at room temperature. Stringent washes for 1 hour were then performed before detection of horse radish peroxidase by Super Signal West Femto Maximum Sensitivity Substrate (Pierce Biotechnology, Rockford, IL) and capture using GeneSnap analysis program (SynGene, MD). Membranes were stripped and re-probed for β-tubulin (Sigma-Aldrich) for normalization of protein levels.

### Co-immunoprecipitation

Keratinocytes (HaCaTs) were used in the immunoprecipitation experiments. Briefly, cells were wounded as described in the scratch assay and allowed to start migrating for 2.5 hours before being washed in PBS, lysed on ice with cell lysis buffer (50 mM Tris, 1 mM EDTA, 50 mM NaCl, 0.1% Triton X-100) supplemented with Protease Inhibitor Complete Mini cocktail tablet (Roche). The cell lysates were precleared by centrifugation, and incubated with 1 μg/1 μl Integrin β1, Integrin β4, CD-151, anti-α-Actinin, anti-Paxillin, anti-Talin and anti-Vinculin antibodies, and protein G-agarose beads (Invitrogen) overnight at 4°C. The immunoprecipitates were collected by centrifugation, pellets washed with lysis buffer, and stored in 2 × sample buffer prior to standard western blotting analysis as previously described. Western Blots were probed with Flii antibody or with Gelsolin antibody as a negative control.

### Co-localization of Flii immunofluorescence

Keratinocytes (HaCaTs) were seeded on glass coverslips, allowed to spread for 6 hours and acetone fixed prior to blocking with 3% NHS for 30 minutes. Cells were incubated with primary antibody (α-Actinin, Paxillin, Vinculin, or Talin) 1:200 dilution overnight at 4°C prior to application of the rabbit Flii primary antibody (1:200) for 1 hour at room temperature. Flii was detected through incubation of cells with fluorescent Alexa Fluor 488 goat anti-rabbit IgG (2 mg ml$^{-1}$) (Invitrogen, OR) whereas actin associated proteins were further detected through species-specific biotinylated secondary antibodies and signal enhancement with Streptavidin Alexa Fluor 555 conjugate (2 mg ml$^{-1}$) (Invitrogen). Coverslips were mounted onto slides using Dako mounting medium. Fluorescence was examined using Leica Spectral confocal microscope.

### Statistical analysis

Statistical differences were determined using the Student's *t*-test or an ANOVA. For data not following a normal distribution, the Mann–Whitney *U*-test was performed. A *P*-value of less than 0.05 was considered significant.

## CONFLICT OF INTEREST

The authors state no conflict of interest.

## ACKNOWLEDGMENTS

This work was supported in part by a grant from the National Health and Medical Research Council of Australia (NHMRC). AJC is supported by an NHMRC career development award. RA is supported by The Sylvia and Charles Viertel Charitable Foundation

## REFERENCES

Adams DH, Strudwick XL, Kopecki Z, Hooper-Jones JA, Matthaei KI, Campbell HD *et al.* (2008) Gender specific effects on the actin-remodelling protein Flightless I and TGF-beta1 contribute to impaired wound healing in aged skin. *Int J Biochem Cell Biol* 40: 1555–69

Arnaout MA, Goodman SL, Xiong JP (2007) Structure and mechanics of integrin-based cell adhesion. *Curr Opin Cell Biol* 19:495–507

Baldwin G, Novitskaya V, Sadej R, Pochec E, Litynska A, Hartmann C *et al.* (2008) Tetraspanin CD151 regulates glycosylation of α3β1 integrin. *J Biol Chem* 283:35445–54

Berrier AL, Yamada KM (2007) Cell-matrix adhesion. *J Cell Physiol* 213:565–73

Brakebusch C, Fassler R (2005) Beta 1 integrin function *in vivo*: adhesion, migration and more. *Cancer Metastasis Rev* 24:403–11

Campbell HD, Fountain S, McLennan IS, Berven LA, Crouch MF, Davy DA *et al.* (2002) Fliih, a gelsolin-related cytoskeletal regulator essential for early mammalian embryonic development. *Mol Cell Bio* 22: 3518–3526

Chometon G, Zhang ZG, Rubinstein E, Boucheix C, Mauch C, Aumailley M (2006) Dissociation of the complex between CD151 and laminin-binding integrins permits migration of epithelial cells. *Exp Cell Res* 312:983–95

Cowin AJ, Adams D, Geary SM, Wright MD, Jones JC, Ashman LK (2006) Wound healing is defective in mice lacking tetraspanin CD151. *J Invest Dermatol* 126:680–9

Cowin AJ, Adams DH, Strudwick XL, Chan H, Hooper JA, Sander GR *et al.* (2007) Flightless I deficiency enhances wound repair by increasing cell migration and proliferation. *J Pathol* 211:572–81

Critchley DR, Holt MR, Barry ST, Priddle H, Hemmings L, Norman J (1999) Integrin mediuated cell adhesion: the cytoskeletal connection. *Biochem Soc Symp* 65:79–99

Davy DA, Ball EE, Matthaei KI, Campbell HD, Crouch MF (2000) The flightless I protein localizes to actin-based structures during embryonic development. *Immunol Cell Biol* 78:423

Defilippi P, Olivo C, Venturino M, Dolce L, Silengo L, Tarone G (1999) Actin cytoskeleton organization in response to integrin-mediated adhesion. *Microsc Res Tech* 47:67–78

DiPersio CM, Hodivala-Dilke KM, Jaenisch R, Kreidberg JA, Hynes RO (1997) alpha3beta1 Integrin is required for normal development of the epidermal basement membrane. *J Cell Biol* 137:729–42

Dogic D, Rousselle P, Aumailley M (1998) Cell adhesion to laminin 1 or 5 induces isoform-specific clustering of integrins and other focal adhesion components. *J Cell Sci* 111:793–802

El Ghalbzouri A, Hensbergen P, Gibbs S, Kempenaar J, van der Schors R, Ponec M (2004) Fibroblasts facilitate re-epithelialization in wounded human skin equivalents. *Lab Invest* 84:102–12

Fassler R, Meyer M (1995) Consequences of lack of beta 1 integrin gene expression in mice. *Genes Dev* 9:1896–908

Fong KS, de Couet HG (1999) Novel proteins interacting with the leucine-rich repeat domain of human flightless-I identified by the yeast two-hybrid system. *Genomics* 58:146–57

Geary SM, Cowin AJ, Copeland B, Baleato RM, Miyazaki K, Ashman LK (2008) The role of the tetraspanin CD151 in primary keratinocyte and fibroblast functions: implications for wound healing. *Exp Cell Res* 314:2165–75

Georges-Labouesse E, Messaddeq N, Yehia G, Cadalbert L, Dierich A, Le Meur M (1996) Absence of integrin α6 leads to epidermolysis bullosa and neonatal death in mice. *Nat Genet* 13:370–3

Gonzalez AM, Otey C, Edlund M, Jones JCR (2001) Interactions of a hemidesmosome component and actinin family members. *J Cell Sci* 114:4197–206

Grose R, Hutter C, Bloch W, Thorey I, Watt FM, Fassler R *et al.* (2002) A crucial role of beta 1 integrins for keratinocyte migration *in vitro* and during cutaneous wound repair. *Development* 129:2303–15

Hehlgans S, Haase M, Cordes N (2007) Signalling via integrins: implications for cell survival and anticancer strategies. *Biochim Biophys Acta* 1775:163–80

Hintermann E, Quaranta V (2004) Epithelial cell motility on laminin-5: regulation by matrix assembly, proteolysis, integrins and erbB receptors. *Matrix Biol* 23:75–85

Hynes RO (2002) Integrins: bidirectional, allosteric signaling machines. *Cell* 110:673–87

Jones JC, Hopkinson SB, Goldfinger LE (1998) Structure and assembly of hemidesmosomes. *Bioessays* 20:488–94

Jaunzems AE, Woods AE, Staples A (1997) Electron microscopy and morphometry enhances differentiation of epidermolysis bullosa subtypes. With normal values for 24 parameters in skin. *Arch Dermatol Res* 289:631–9

Kaibuchi K, Kuroda S, Amano M (1999) Regulation of the cytoskelton and cell adhesion by the Rho family GTPases in mammalian cells. *Annu Rev Biochem* 68:459–86

Kirfel G, Herzog V (2004) Migration of epidermal keratinocytes: mechanisms, regulation, and biological significance. *Protoplasma* 223:67–78

Kopecki Z, Cowin AJ (2008) Flightless I: An actin-remodelling protein and an important negative regulator of wound repair. *Int J Biochem Cell Biol* 40:1415–9

Lee YH, Campbell HD, Stallcup MR (2004) Developmentally essential protein flightless I is a nuclear receptor coactivator with actin binding activity. *Mol Cell Biol* 24:2103–17

Lee YH, Stallcup MR (2006) Interplay of Fli-I and FLAP1 for regulation of beta-catenin dependent transcription. *Nucleic Acids Res* 34:5052–9

Litjens SHM, de Pereda JM, Sonnenberg A (2006) Current insights into the formation and breakdown of hemidesmosomes. *Trends Cell Biol* 16:376–83

Liu L, He B, Liu WM, Zhou D, Cox JV, Zhang XA (2007) Tetraspanin CD151 promotes cell migration by regulating integrin trafficking. *J Biol Chem* 282:31631–42

Mainiero F, Murgia C, Wary KK, Curatola AM, Pepe A, Blumemberg M *et al.* (1997) The coupling of α6β4 integrin to Ras-MAP kinase pathways mediated by Sch controls keratinocyte proliferation. *EMBOJ* 16:2365–75

Manohar A, Shome SG, Lamar J, Stirling L, Iyer V, Pumiglia K *et al.* (2004) α3β1 integrin promotes keratinocyte cell survival through activation of a MEK/ERK signaling pathway. *J Cell Sci* 117:4043–54

May AL, Wood FM, Stoner ML (2001) Techniques: Assessment of adhesion assays for use with keratinocytes. *Exp Dermatol* 10:62–9

Nguyen BP, Ryan MC, Gil SG, Carter WG (2000) Deposition of laminin 5 in epidermal wounds regulates integrin signaling and adhesion. *Curr Opin Cell Biol* 12:554–62

Peltonen J, Larjava H, Jaakkola S, Gralnick H, Akiyama SK, Yamada SS *et al.* (1989) Localization of integrin receptors for fibronectin, collagen, and laminin in human skin. Variable expression in basal and squamous cell carcinomas. *J Clin Invest* 84:1916–23

Raymond K, Kreft M, Janssen H, Calafat J, Sonnenberg A (2005) Keratinoctyes display normal proliferation, survival and differentiation in conditional β4-integrin knockout mice. *J Cell Sci* 118: 1045–1060

Redvers PR, Kaur P (2004) Epidermal Cells: Methods and Protocols—Serial Cultivation of Primary Adult Murine Keratinocytes. *Methods Mol Biol* 289:15–22

Reynolds LE, Conti FJ, Silva R, Robinson SD, Iyer V, Rudling R *et al.* (2008) α3β1 integrin - controlled Smad7 regulates reepithealialization during wound healing in mice. *J Clin Invest* 118:965–74

Santoro MM, Gaudino G (2005) Cellular and molecular facets of keratinocyte reepithelization during wound healing. *Exp Cell Res* 304:274–86

Sincock PM, Fitter S, Parton RG, Berndt MC, Gamble JR, Ashman LK (1999) PETA-3/CD151, a member of the transmembrane 4 superfamily, is localised to the plasma membrane and endocytic system of endothelial cells, associates with multiple integrins and modulates cell function. *J Cell Sci* 112:833–44

Watt FM (2002) Role of integrins in regulating epidermal adhesion, growth and differentiation. *EMBO J* 21:3919–26

Wipff PJ, Hinz B (2008) Integrins and the activation of latent transforming growth factor β1 - An intimate relationship. *Eur J Cell Biol* 87: 601–15

Zhang X, Jiang G, Cai Y, Monkeley SJ, Critchley DR, Sheetz MP (2008) Talin depletion reveals independence of initial cell spreading from integrin activation and traction. *Nat Cel Biol* 10:1062–8